Responses to the comments of Reviewer #1:

We would like to thank the anonymous referee for his/her comprehensive review and valuable suggestions. These suggestions help us to present our results more clearly. In response, we have made changes according to the referee's suggestions and replied to all comments point by point. All the page and line number for corrections are referred to the revised manuscript, while the page and line number from original reviews are kept intact.

General comments

1. The study uses the MEIC v1.4 2019 inventory as the prior for a winter 2022-2023 inversion and concludes that MEIC systematically underestimates winter emissions by 16.1%. However, China's fossil CO_2 emissions rose by ~10% from 2019 to 2022 and ~14% to 2023 (Friedlingstein et al., 2026), with even larger increases in coal, which dominates winter heating. A substantial fraction of the 16.1% difference may reflect real emission growth rather than a structural inventory bias. Please clarify this point.

Response: We appreciate the reviewer for this insightful comment. We agree that the 16.1% increase in posterior emissions relative to the MEIC v1.4 2019 prior may reflect both actual emission growth between 2019 and winter 2022–2023 and systematic biases in the inventory. Therefore, this difference cannot be attributed entirely to systematic underestimation by MEIC, and our current analysis does not separately quantify these contributions.

We have revised the relevant discussion to clarify this point. We have also replaced references to MEIC overestimation or underestimation with descriptions of posterior decreases or increases relative to the prior throughout the manuscript.

See Lines 388–396, Page 13.

"...Compared with the MEIC v1.4 2019 prior, the posterior emissions exhibited an overall upward adjustment at the national scale. Total posterior anthropogenic CO_2

emissions during the winter period amounted to 2808.3 ± 257.7 Tg, 16.1% higher than the MEIC v1.4 2019 prior. This difference may reflect both inventory biases and actual emission growth since 2019. According to the Global Carbon Budget, China's annual fossil CO_2 emissions in 2022 and 2023 were approximately 10% and 14% above 2019 levels, respectively, with larger increases in coal-related emissions (Friedlingstein et al., 2026). Such growth is relevant to wintertime emission adjustments, particularly in northern China, where coal is a major fuel for heating."

See Lines 400–403, Page 13.

"The adjustments of posterior CO_2 emissions exhibited distinct spatial heterogeneity, with emission increases mainly located in northern China, particularly in the North China Plain. These increases may partly reflect changes in heating-related emissions between 2019 and winter 2022–2023, as well as potential biases in the prior inventory."

See Lines 428–431, Page 15.

"The total posterior emissions for the YRD were 345.9 ± 64.3 Tg, 10.4% lower than the MEIC v1.4 2019 prior. This difference may reflect changes in regional winter emissions since 2019 and overestimated emission factors in the prior inventory."

See Lines 609–621, Pages 24–25.

"The prior simulation exhibits a positive bias relative to observations, especially during high CO_2 episodes (Fig. 4g), which is consistent with the posterior emission decrease relative to the prior in this region. Following optimization, the posterior simulation effectively reduces this positive concentration bias. Although the posterior simulation retains a residual negative bias, primarily attributable to the spatial representation error between grid-mean model concentrations and point-scale urban measurements heavily impacted by intense local emissions (Tolk et al., 2008), the MAE and RMSE decrease by 21.9% and 25.2%, respectively, while the CORR slightly increases from 0.56 to 0.58.

This marked reduction in positive concentration bias provides compelling evidence that the system can robustly constrain emissions even in urban regions characterized by dense anthropogenic sources."

2. Individual OCO-2/3 sounding retrieval errors are not independent. Baker et al. (2022) showed that along-track OCO-2 errors exhibit spatial correlation scales of ~10 km and ~20 km. This study uses per-sounding XCO_2 uncertainties as the observation error. Assimilating multiple correlated soundings within a 27 km grid cell may overestimate the effective observational constraint and lead to overfitting. Please clarify whether the data have been aggregated along-track (e.g., 10-second averages) or whether error correlations have been accounted for.

Response: Thank you for this valuable comment. We agree that individual OCO-2/3 retrieval errors can be spatially correlated and that assimilating closely spaced soundings as independent observations may overestimate the effective observational constraint. The approximately 10 and 20 km along-track error correlation scales reported by Baker et al. (2022) underscore this concern. In this study, we did not assimilate all individual soundings directly; instead, we aggregated them into super-observations before assimilation. Specifically, we first screened the soundings according to the 3-day assimilation window and then averaged their XCO_2 values within each 27 km model grid cell. The uncertainty assigned to each super-observation was the arithmetic mean of the reported sounding uncertainties. Each aggregation group thus contributed a single observation to the assimilation. Similar procedures have been used in previous satellite CO_2 inversion studies. Jiang et al. (2022) calculated daily arithmetic means of quality-filtered GOSAT XCO_2 retrievals within each 1° × 1° grid cell and averaged the reported retrieval uncertainties in the same way. Byrne et al. (2024) similarly formed OCO-2 super-observations by taking the equal-weight average of soundings within the same orbit and 0.5° × 0.5° grid cell. These studies provide methodological support for grid-level aggregation before assimilation.

We have clarified the preprocessing procedure and observation error assignment

in the revised manuscript. See Lines 310–318, Pages 10-11.

"Nearby OCO-2/3 soundings can have correlated retrieval errors, with OCO-2 along-track error correlation scales of approximately 10 and 20 km reported by Baker et al. (2022). We therefore aggregated these soundings before assimilation. After screening them according to the assimilation time window, we averaged the XCO_2 values within each 27 km model grid cell to form a single super-observation (Jiang et al., 2022; He et al., 2023; Byrne et al., 2024). For the EnSRF assimilation, the observation error standard deviation for each super-observation was estimated based on the reported retrieval uncertainties of the contributing soundings (Jiang et al., 2022). The spatial distribution and counts of the super-observations are shown in Fig. 3."

3. The OSSE uses a spatially uniform 30% reduction of MEIC as the prior, but one of the key findings "downward adjustment in city centers and upward adjustment in suburbs" is a spatially resolved bias that this design cannot test. In fact, Fig. 3 shows that the OSSE inversion derives correction factors with substantial spatial variations, despite a uniform 30% difference between "true" and prior. This suggests that results for small regions (e.g., from a city) should be interpreted with caution. I'd suggest that the authors have some discussion this limitation.

Response: We thank the reviewer for this insightful comment. We agree that the spatially uniform 30% reduction applied to the MEIC inventory in the OSSE represents an idealized prior error structure and does not explicitly account for spatially heterogeneous emission biases, such as overestimations in urban centers and underestimations in surrounding suburban areas.

The primary purpose of this OSSE was to evaluate the capability of RegGCAS to correct a prescribed emission bias under the actual spatial sampling characteristics of OCO-2/3 observations. As you correctly pointed out, despite the spatially uniform relative bias in the prior emissions, the inversion produced spatially varying correction factors (Fig. 3). This behavior can be attributed to spatial differences in observational

coverage, atmospheric transport sensitivity, and the background error covariance structure. Consequently, the inversion may constrain regional emission totals more effectively than individual grid-cell emissions.

To further assess the ability of the inversion system to correct spatially heterogeneous emission biases, we conducted an additional OSSE with spatially heterogeneous prior errors. The prior was constructed by adding spatially varying Gaussian noise to 70% of MEIC emissions, with a standard deviation equal to 25% of MEIC emissions at each grid cell. All other settings remained unchanged. As shown in Fig. S7, the inversion generally reduced the widespread underestimation over eastern China, although substantial biases remained in some grid cells. Absolute errors in regional emission totals decreased by 66.6%, 95.6%, and 59.1% over mainland China, BTH, and the YRD, respectively. These reductions were comparable to those in the original OSSE (67.8%, 98.7%, and 57.9% for mainland China, BTH, and the YRD, respectively). Posterior totals differed from the original results by less than 1% in all three regions. These results indicate that the inversion remained effective in improving emission estimates after spatially heterogeneous prior errors were introduced. Although it does not directly validate the opposing emission adjustments in city centers and suburban areas, the additional experiment provides some evidence that the inversion can correct spatially heterogeneous biases. Limited observational coverage in some areas may also introduce uncertainty into the interpretation of fine-scale spatial patterns in the actual inversion.

Nevertheless, the broadly consistent spatial adjustment patterns obtained from the NO_2-proxy inversion (Fig. 2), which uses independent surface NO_2 observations, provide additional qualitative support for the urban–suburban differences identified from XCO_2 assimilation.

Following the reviewer's suggestion, we have expanded the discussion of this limitation in Section 3.2 and clarified that the urban–suburban adjustment patterns should be interpreted with caution. We have also moderated the relevant conclusions to avoid overstating the capability of the current inversion framework to resolve local

emission allocation biases. Future studies incorporating spatially heterogeneous prior errors in OSSEs and additional high-density observations will be necessary to further evaluate the reliability of these fine-scale adjustments. See Lines 534-548, Page 20. The additional OSSE experiment is described in the Supplement.

"Additionally, grid-cell correction factors varied substantially even when the prior relative bias was spatially uniform (Fig. 3c). Differences in observational coverage and atmospheric transport sensitivity, together with the prescribed background error covariance structure, can contribute to uneven emission recovery across cities and grid cells.

We also conducted an additional OSSE by adding grid-cell Gaussian noise to the original prior emissions (Text S4). Absolute errors in regional emission totals decreased by 66.6%, 95.6%, and 59.1% over mainland China, BTH, and the YRD, respectively, comparable to the reductions in the original OSSE. Posterior totals differed by less than 1% between experiments in all three regions (Fig. S7). The additional OSSE provides further evidence that the inversion can improve emission estimates under spatially heterogeneous prior errors. However, its random perturbations did not specifically represent systematic biases of opposite signs in urban centers and surrounding suburbs, limiting its ability to evaluate the recovery of such contrasting biases. Limited observational coverage in some areas may also introduce uncertainty into the interpretation of the urban–suburban adjustment patterns identified in the actual inversion."

See Lines 754-757, Page 31.

"Conversely, emissions in the YRD were adjusted downward by 10.4%, reflecting positively biased emission factors in MEIC. Spatially, posterior emissions showed localized decreases in some urban centers and increases in parts of the surrounding areas."

See Lines 780-785, Page 32.

"Moreover, the distinct urban-suburban correction pattern highlights the limitations of proxy-based downscaling in current gridded inventories, which frequently allocate excessive emissions to urban cores while underestimating major industrial sources in suburban belts. However, limited observational coverage may introduce substantial uncertainty into the interpretation of fine-scale spatial patterns."

"**Supplement**

Text S4. OSSE with spatially heterogeneous prior emission errors

To assess the sensitivity of emission recovery to spatially heterogeneous prior errors, we conducted an additional OSSE by adding grid-cell Gaussian noise to the prior emissions used in the original experiment. The perturbed prior emissions were constructed as:

$$E_{prior,i} = 0.70E_{MEIC,i} + 0.25E_{MEIC,i}\xi_i, \qquad \xi_i \sim N(0,1).$$

Where $E_{prior,i}$ denotes the perturbed prior emissions in grid cell i, $E_{MEIC,i}$ denotes the corresponding MEIC emissions, and ξ_i is a standard normally distributed random variable. The coefficient 0.25 sets the standard deviation of the perturbation to 25% of the MEIC emissions in each grid cell.

The inversion generally reduced the widespread negative emission biases over eastern China, although substantial residual biases remained in some grid cells (Fig. S7). Absolute errors in regional emission totals decreased by 66.6%, 95.6%, and 59.1% over mainland China, BTH, and the YRD, respectively. These reductions were comparable to those in the original OSSE (68.0%, 98.7%, and 58.0%, respectively). Posterior emission totals differed by less than 1% between the two experiments in all three regions, indicating that regional estimates were relatively insensitive to the tested grid-cell perturbations."

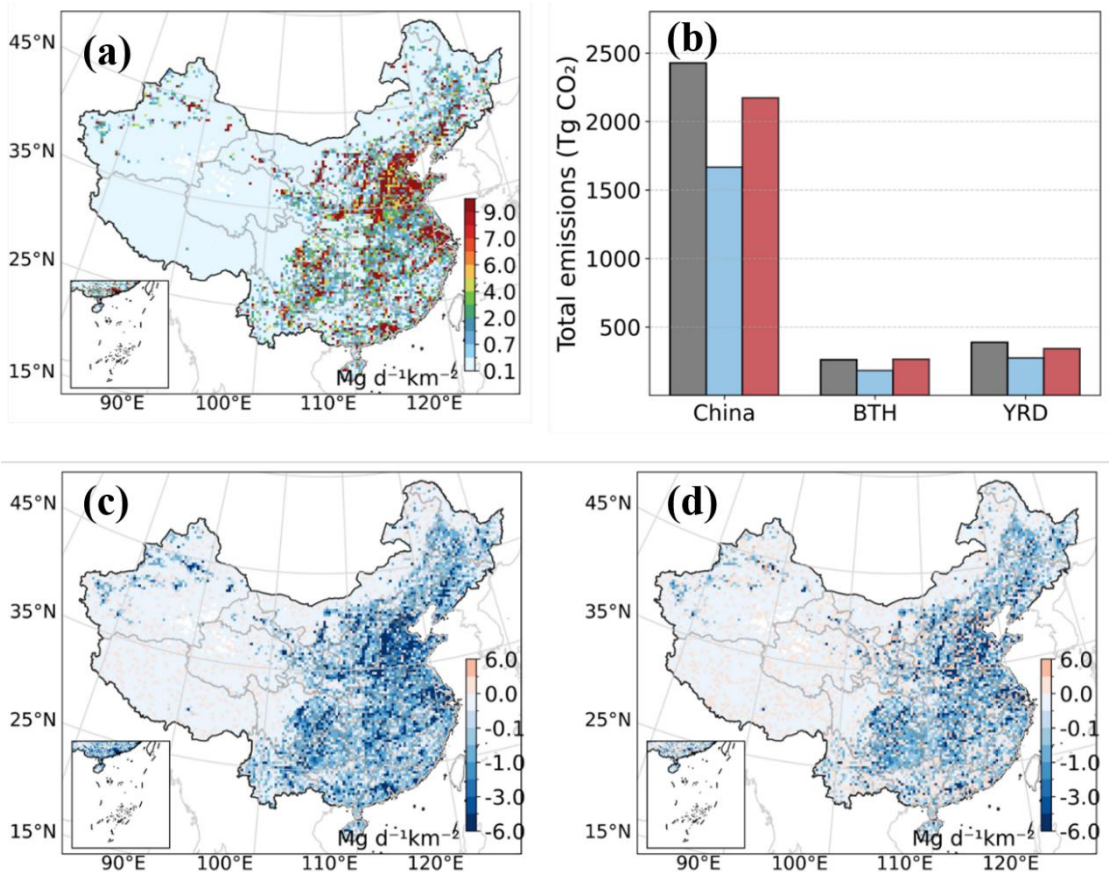


Figure S7 Results of the OSSE with spatially heterogeneous prior errors: (a) posterior CO_2 emissions, (b) regional emission totals for the truth, prior, and posterior, (c) prior minus true emissions, and (d) posterior minus true emissions.

Specific comments

1. Line 36-39 and Line 584-586: The improvement against assimilated OCO-2/3 observations is an internal consistency diagnostic, not an independent validation. The Methods section correctly distinguishes between the two, but the Abstract and Conclusions list the OCO-2/3 fit alongside TCCON, ObsPack, and the urban site as if they were equivalent validations. Please correct this.

Response: We appreciate the reviewer for this helpful comment. We agree that the improved agreement with the assimilated OCO-2/3 observations represents an internal consistency diagnostic rather than an independent validation. We have therefore revised

both sections to distinguish the fit to assimilated observations from validation against independent TCCON, ObsPack, and urban site observations.

We have revised the relevant descriptions in the Abstract and Conclusions as follows. See Lines 36–41, Page 2.

"**Abstract:** ...Evaluation demonstrates that assimilation effectively reduces prior emission errors by 68.0%. As an internal consistency diagnostic, the posterior simulations show a 5.8% reduction in RMSE against the assimilated OCO-2/3 XCO2 observations. Independent validation against TCCON, ObsPack, and urban site observations shows RMSE reductions of 15.3%, 7.7%, and 25.2%, respectively, confirming the enhanced accuracy of the posterior emission estimates."

See Lines 764–769, Page 31.

"4. Summary and conclusions

Furthermore, posterior simulations reduced the RMSE against assimilated OCO-2/3 XCO_2 observations by 5.8%, indicating improved internal consistency. Independent validation against TCCON XCO_2, ObsPack surface CO_2, and dedicated high-precision urban site observations showed RMSE reductions of 15.3%, 7.7%, and 25.2%, respectively, supporting improved simulated concentrations and lending further confidence to the posterior emission estimates."

2. Line 104-105: The text states that winter biogenic fluxes in the YRD account for only 0.2% of anthropogenic emissions, yet the BIO_CASA sensitivity experiment (Table 2) shows an 11.7% change in posterior anthropogenic emissions when switching the biogenic flux product. Please explain why biogenic fluxes that are small in absolute magnitude have such a large impact on the inversion.

Response: Thank you for this comment. The approximately 0.2% cited in the original

text comes from Zhang et al (2024). It refers to the magnitude of the BEPS-derived net biospheric flux relative to anthropogenic emissions in the YRD in December 2020. This ratio is specific to that product and period. We acknowledge that our wording did not clearly define its scope. It could therefore imply that winter biospheric fluxes and their uncertainties are negligible.

To clarify this issue, we compared the biospheric net fluxes and the anthropogenic emissions in BASE and BIO_CASA (Table S1). The magnitudes of the BEPS prior net fluxes account for only 0.3%, 0.1%, and 0.2% of prior anthropogenic emissions over mainland China, BTH, and the YRD, respectively. However, these small proportions are specific to BEPS. Over mainland China, the prior biospheric net flux changes from −2.1 Tg CO_2 $month^{-1}$ with BEPS to 340.8 Tg CO_2 $month^{-1}$ with CASA. This difference of 342.9 Tg CO_2 $month^{-1}$ is equivalent to 42.5% of prior anthropogenic emissions. The corresponding differences in BTH and the YRD are equivalent to 13.4% and 23.2% of their respective prior anthropogenic emissions. Thus, replacing BEPS with CASA introduces a substantial change in the biospheric prior, despite the small net fluxes represented by BEPS. This change is accompanied by an 11.7% decrease in national posterior anthropogenic emissions, from 936.1 to 826.5 Tg CO_2 $month^{-1}$.

With other experimental settings unchanged, the larger net biospheric release in BIO_CASA increases the CO_2 input to the atmosphere. Atmospheric transport carries this additional CO_2 to the observation locations, changing the simulated XCO_2 and the model–observation differences used in the assimilation. These changes affect the anthropogenic emission updates, resulting in lower posterior anthropogenic emissions in BIO_CASA. The 11.7% decrease therefore reflects the substantial difference between the two biospheric priors, rather than a large response to a small biospheric flux.

We have removed the cited 0.2% estimate to avoid generalizing a product- and period-specific result. We have also added the comparison in Table S1 and expanded the discussion of how biospheric product differences affect anthropogenic emission estimates. See Lines 107–115, Page 4.

Table S1 Mean monthly biospheric net CO_2 fluxes and anthropogenic CO_2 emissions in the BEPS and CASA experiments (Tg CO_2 $month^{-1}$).

Region	Type	Bio	Anth_prior	Anth_post
China	BEPS	-2.1	806.4	936.1
	CASA	340.8	806.4	826.5
BTH	BEPS	0.1	86.7	98.1
	CASA	11.7	86.7	83.7
YRD	BEPS	-0.3	128.7	115.3
	CASA	29.5	128.7	99.3

"Winter offers favorable conditions for constraining anthropogenic CO_2 emissions, as reduced biospheric activity limits interference from biospheric CO_2 signals (Zhang et al., 2024b). Regional carbon assimilation systems provide a framework for constraining these emissions using atmospheric CO_2 observations. Using the regional carbon assimilation system RegGCAS (Feng et al., 2025), Zhang et al. (2024b) inverted anthropogenic CO_2 emissions in the YRD during winter by assimilating ground-based CO_2 observations, demonstrating the potential of this approach to reduce uncertainties in prior emission estimates. Nevertheless, uncertainties in biospheric CO_2 fluxes may still affect anthropogenic emission estimates, even during winter (Basu et al., 2016; Wu et al., 2018)."

See Lines 670–688, Page 27.

"In the biospheric flux sensitivity experiment (BIO_CASA), posterior anthropogenic emissions decreased by 11.7% relative to BASE. This decrease was primarily associated with substantial differences between the two biospheric products (Table S1). The national prior biospheric net fluxes were −2.1 and 340.8 Tg CO_2 $month^{-1}$ for BEPS and CASA, respectively. Their difference of 342.9 Tg CO_2 $month^{-1}$ was equivalent to 42.5% of prior anthropogenic emissions. The larger positive biospheric fluxes in CASA

were particularly evident over central-eastern, North China, and Northeast China regions, thereby elevating the natural background CO_2 levels. To match satellite XCO_2 observations, the assimilation system offsets this higher biogenic background by producing correspondingly lower posterior anthropogenic emissions. These results indicate that the choice of biospheric prior affects the magnitude of anthropogenic emission adjustments through its contribution to simulated XCO_2. The 11.7% decrease in BIO_CASA highlights the importance of this uncertainty for winter anthropogenic CO_2 emission estimates."

3. Line 256-278: Please describe the spatiotemporal collocation methods used to compare model output with TCCON, ObsPack, and the ZJ urban site.

Response: We thank the reviewer for this helpful suggestion. We acknowledge that the spatiotemporal collocation procedures were not clearly described in the original manuscript. For comparisons with TCCON, ObsPack, and ZJ observations, we selected the model grid cell whose center was closest to each station. Observations were then matched with the corresponding hourly model output. For vertical matching, model CO_2 profiles were linearly interpolated to the TCCON pressure levels. Simulated XCO_2 was then calculated using the TCCON a priori profiles and column averaging kernels to account for the vertical sensitivity of the retrievals (Rodgers and Connor, 2003). For ObsPack, model layer heights and observation altitudes were expressed relative to sea level, and model CO_2 concentrations were linearly interpolated to the reported observation altitude to compare them with the observations (Agustí-Panareda et al., 2014). For the ZJ site, we used CO_2 concentrations from the lowest model layer for comparison based on the site's height.

We have clarified these procedures in the revised manuscript. See Lines 342–354, Page 11-12.

"... The spatial distribution of all validation sites is shown in Fig. 2a. Model output was collocated with these sites before evaluation. Spatially, CO_2 concentrations were

extracted from the model grid cell whose center was closest to each site. Temporally, each observation was matched to the mean model output for the hour in which it was recorded. For vertical matching, model CO_2 profiles were linearly interpolated in log pressure to the TCCON pressure levels. Simulated XCO_2 was then calculated by pressure-weighted integration incorporating the TCCON a priori profiles and column averaging kernels (Rodgers and Connor, 2003). For ObsPack, model layer heights were converted to altitude above sea level, and CO_2 concentrations were linearly interpolated to the reported observation altitude for comparison (Agustí-Panareda et al., 2014). For ZJ, CO_2 concentrations from the lowest model layer were used for comparison based on the site's height. Moreover, the evaluation metrics included mean bias (BIAS), mean absolute error (MAE), root mean square error (RMSE), and correlation coefficient (CORR).”

4. Line 379-381: I do not agree that the two methods are consistent in BTH based on Fig. 2. Reporting regional totals and also time series may help a reader. In addition, how interference of biogenic fluxes affects the inference on anthropogenic emissions. This is a key question that is not adequately discussed.

Response: Thank you for this comment. We agree that the two methods do not yield consistent anthropogenic CO_2 emission estimates in BTH. The lower emissions from the original proxy inversion were related to the CO_2-to-NO_X emission ratios used in the conversion. Because of the time lag in updating bottom-up inventories, we used ratios from the 2019 MEICv1.4 inventory. Previous studies have reported increasing CO_2-to-NO_X ratios over East Asia (Li et al., 2024; Li et al., 2023), potentially with a stronger increase in BTH under stringent winter pollution controls (Xu et al., 2023; Liu et al., 2020). Our comparison shows that the ratios from MEICv2 for winter 2022–2023 were substantially higher than those for winter 2019–2020 (Fig. R1). Using the 2019 ratios therefore underestimated the proxy-derived CO_2 emissions. We have recalculated the proxy inversion using the winter 2022–2023 ratios from MEICv2. Fig. S6 presents the

updated emission time series. Using the revised CO_2-to-NO_X ratios, we also updated the YRD estimates. The XCO_2-based posterior estimates were lower than the proxy estimates, as limited satellite coverage provided weaker observational constraints in this region. We have updated the proxy inversion results and related discussion throughout the revised manuscript.

Biospheric fluxes affect simulated XCO_2 and thus the model–observation differences used to optimize anthropogenic emissions. Greater biospheric release or weaker uptake may be compensated for by lower inferred anthropogenic emissions, and vice versa. Although our system jointly optimizes anthropogenic and biospheric fluxes, CO_2 observations constrain their combined atmospheric signal and provide limited ability to distinguish their contributions within the same grid cell. Uncertainties in biospheric fluxes can therefore introduce substantial errors into anthropogenic emission estimates. We have clarified this influence in the revised manuscript.

See Lines 472–492, Page 16.

"This study also estimates anthropogenic CO_2 emissions using a NO_2-proxy method, with monthly CO_2-to-NO_X emission ratios from MEICv2 for December 2022–February 2023 (Fig. 2). In BTH, both methods yield relatively high emissions in southern Hebei and the Beijing–Tianjin–Tangshan area and lower emissions in northern Hebei. The main emission adjustments occur near major cities and their surrounding areas, with decreases near many urban centers and increases in parts of the surrounding areas. Compared with direct XCO_2 assimilation, the NO_2-proxy method produces more extensive decreases around Beijing and Tianjin and stronger increases in parts of central and southern Hebei. These differences may partly reflect uncertainties in the CO_2-to-NO_X emission ratios, which depend on sectoral composition and pollution control technologies (Miyazaki and Bowman, 2023; Li et al., 2023). In the YRD, both methods showed emission decreases around southern Jiangsu and Shanghai, with localized reductions also occurring in parts of Zhejiang. Similar urban–suburban adjustment patterns were observed, as in the BTH region. However, the NO_2-proxy method

produced more pronounced spatial adjustments and yielded a higher regional emission total than direct XCO_2 assimilation. Satellite XCO_2 observations were available in only 14 assimilation windows over the YRD, fewer than half of the total, providing limited temporal coverage for constraining regional emissions. By comparison, observations covered 70% of the assimilation windows in BTH, where the two methods yielded closer regional emission totals. Overall, the comparison provides additional qualitative support for the emission adjustment patterns in key regions and highlights the need for more observational constraints in the YRD."

See Lines 679–688, Page 27.

"…To match satellite XCO_2 observations, the assimilation system offsets this higher biogenic background by producing correspondingly lower posterior anthropogenic emissions. These results indicate that the choice of biospheric prior affects the magnitude of anthropogenic emission adjustments through its contribution to simulated XCO_2. Although anthropogenic and biospheric fluxes are jointly optimized, satellite XCO_2 observations constrain their combined atmospheric signal, limiting the separation of their contributions within the same grid cell. Consequently, uncertainties in biospheric fluxes can propagate into anthropogenic emission estimates even under joint optimization. The 11.7% decrease in BIO_CASA highlights the importance of this uncertainty for winter anthropogenic CO_2 emission estimates."

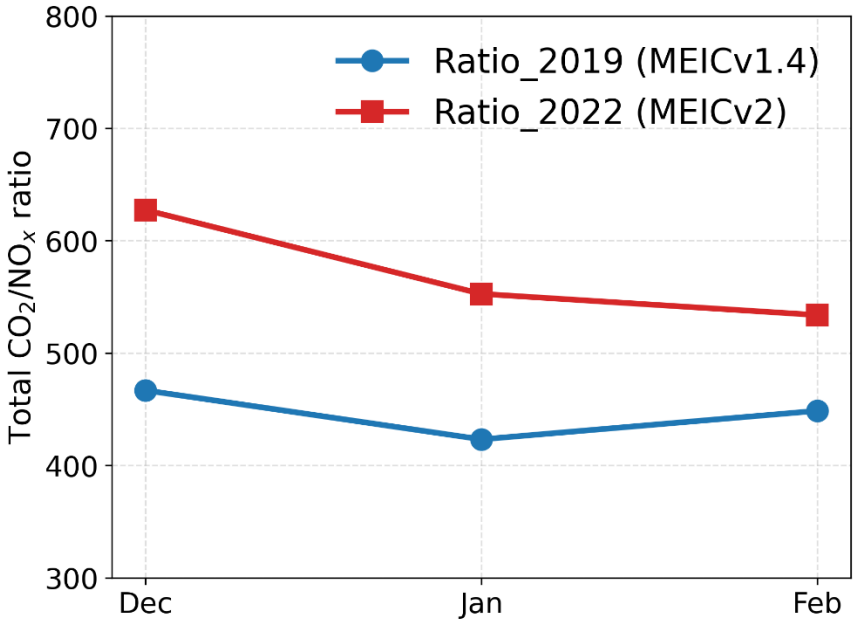


Figure R1 Comparison of monthly CO_2/NO_X ratios in the BTH region between winter 2019–2020 and winter 2022–2023.

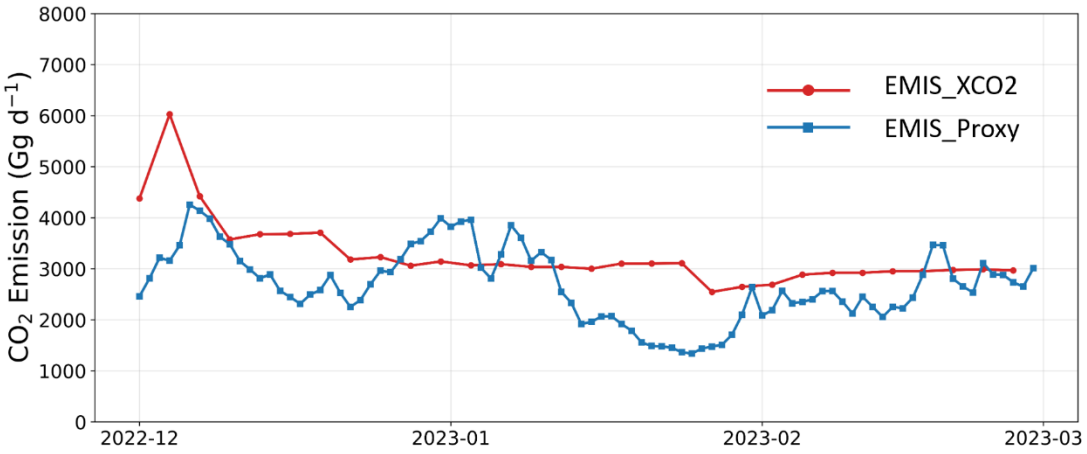


Figure S6 Anthropogenic CO_2 emission time series in BTH from XCO_2 assimilation and the NO_2-proxy method using MEICv2 ratios for winter 2022–2023.

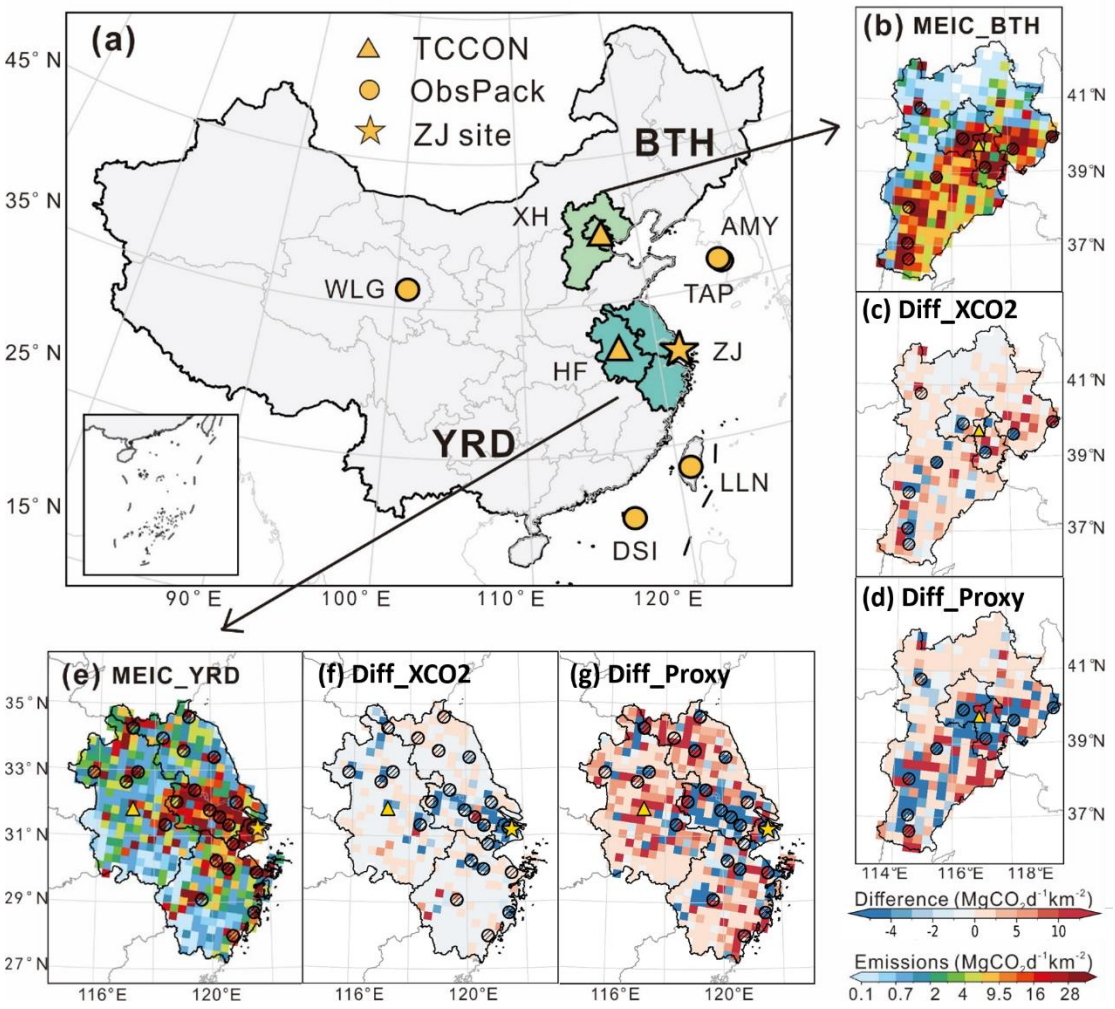


Fig. 2. Spatial distribution of emissions and adjustments ($MgCO_2\ d^{-1}\ km^{-2}$) in the BTH and YRD regions. (a) BTH and YRD locations. Yellow circles denote ObsPack sites; (b-d) BTH: posterior emissions, and emissions adjustments derived from direct XCO_2 assimilation (Diff_XCO_2) and the NO_2-proxy method (Diff_Proxy), respectively; (e-g) same as (b-d) but for YRD. The yellow triangle denotes the XH site (b-d) and HF site (e-g). The yellow five-pointed star denotes the ZJ site. Hatched circles denote key city centers.

5. Line 382-394: Posterior emissions show a marked drop during the Spring Festival (Fig. 1f), while the prior has only monthly-mean temporal resolution. Could part of this signal arise from meteorological variations during the holiday period, rather than from emission changes alone?

Response: We thank the reviewer for this comment. The monthly temporal resolution applies to the prior emissions, whereas CO_2 transport and mixing are simulated using hourly meteorological fields. Therefore, meteorological influences on atmospheric CO_2 transport and dispersion, including changes in wind fields and boundary-layer mixing, are explicitly represented in the forward simulations. The emission–concentration relationships used in the inversion are established under these time-varying meteorological conditions, allowing the effects of simulated meteorological variability on atmospheric CO_2 concentrations to be accounted for when estimating emissions. Consequently, the inversion minimizes the discrepancies between simulated and observed XCO_2 primarily by correcting prior emission errors. Thus, the posterior emission variations are expected to primarily reflect changes in anthropogenic activities rather than meteorological variability. The 3-day assimilation window allows posterior emissions to capture short-term variations absent from the monthly prior inventory.

Nevertheless, uncertainties in the representation of atmospheric transport and boundary-layer mixing may still propagate into the inferred emissions. To further examine the influence of meteorology-driven transport differences, we conducted a sensitivity experiment replacing the FNL meteorological forcing with ERA5. Posterior anthropogenic CO_2 emissions over mainland China increased from 2808.3 to 2945.3 Tg, a difference of 137.0 Tg (4.9%). Although the ERA5-driven estimates were generally higher, both experiments captured an emission decrease during the Spring Festival (Fig. S8). This agreement suggests that the inferred holiday decrease is robust to the tested change in meteorological forcing and supports its interpretation as reflecting reduced holiday activity.

We have added this sensitivity experiment to Section 3.3, “System sensitivity and uncertainty assessment”. See Lines 702–710, Pages 29–30.

“Uncertainties in atmospheric transport can contribute to model–observation mismatches. In particular, errors in meteorological fields, such as winds and boundary-layer mixing, can alter the horizontal transport and vertical redistribution of CO_2,

affecting the source–receptor relationships linking surface emissions to observed XCO_2. These transport-related mismatches may then be compensated for through emission adjustments, thereby influencing the inferred CO_2 emissions (Basu et al., 2018; Schuh et al., 2019). To assess this sensitivity, we replaced FNL with ERA5 meteorological forcing (MET_ERA5). Posterior anthropogenic CO_2 emissions over mainland China increased from 2808.3 to 2945.3 Tg (+4.9% relative to BASE)."

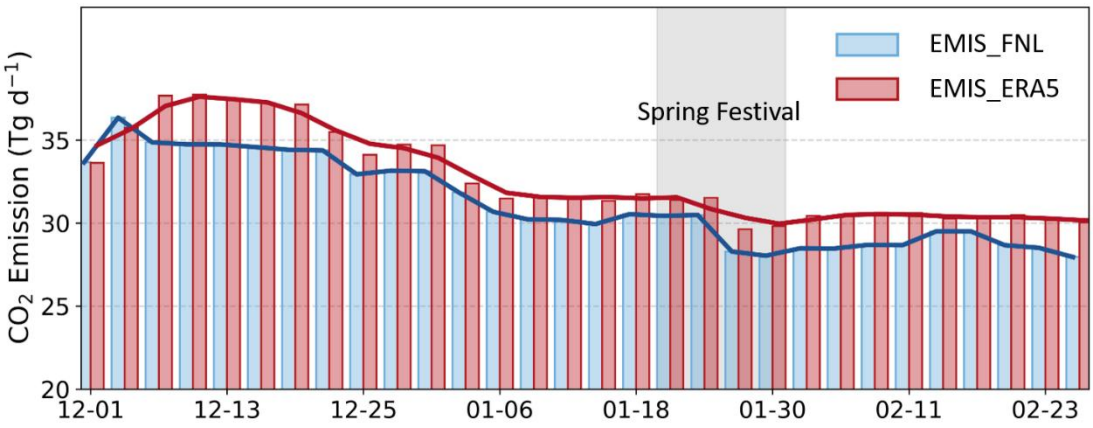


Figure S8 Time series of posterior anthropogenic CO_2 emissions over mainland China using FNL and ERA5 meteorological forcing during winter 2022–2023. The shaded area indicates the Spring Festival holiday.

6. Line 609-610: The statement "the inherent structural biases identified within the bottom-up inventories are likely applicable throughout the year" is not sufficiently supported by winter-only results. Please soften this claim.

Response: We appreciate the reviewer for this helpful comment. We have removed this inference and revised the conclusions to explicitly limit the findings to the study period while emphasizing the need for future multi-season inversions. See Lines 799–806, Pages 32–33.

"...Finally, this study focused on winter 2022-2023, and whether the discrepancies identified between posterior estimates and bottom-up inventories persist in other seasons remains uncertain. Future work should extend the inversions to other seasons

and evaluate the results against independent observations. Joint assimilation of surface and satellite observations, along with carbon isotope measurements where available, could help better distinguish anthropogenic emissions from natural CO_2 fluxes, thereby extending reliable top-down emission constraints to an annual scale."

7. Fig. 4g: Just a comment: I appreciate that the authors evaluate the posterior simulation against the ZJ site located within the source region. This is valuable.

Response: Thank you very much for your positive comment.

Technical corrections

1. Line 36-37: decrease -> decreases

Response: We have changed "decrease" to "decreases". See Line 38, Page 2.

2. Line 244: "(Taylor et al., 2023) reported" -> "Taylor et al. (2023) reported".

Response: We have changed "(Taylor et al., 2023) reported" to "Taylor et al. (2023) reported". See Line 301, Page 10.

3. Line 314: Which months are included as winter?

Response: Thank you for pointing out this ambiguity. In this study, "winter" refers to the three-month period of December 2022, January 2023, and February 2023 (i.e., the boreal winter season). This definition is consistent with the temporal coverage of our inversion period.

We have clarified the definition of winter directly in the revised manuscript. See Lines 128-131, Page 5.

"Given the sparse ground-based observations and biogenic signal interference in regional anthropogenic CO_2 inversion, this study integrates OCO-2/3 XCO_2

observations into RegGCAS to invert national anthropogenic CO_2 emissions during winter 2022-2023 (i.e., December 2022 to February 2023)."

4. Line 342: "overestimated" -> "overestimation".

Response: We have replaced "overestimation" with "decrease" to describe the posterior–prior difference without attributing it directly to inventory bias. See Line 428-429, Page 15.

"Total posterior emissions for the YRD were 345.9 ± 46.3 Tg, representing a 10.4% decrease relative to the MEIC v1.4 2019 prior."

5. Line 364: A little bit of ambiguity on "the proxy-based method", as you have just mentioned "proxy variables" in the last paragraph. Better to describe the method with clearer language (maybe "anthropogenic CO_2 emissions from the NO_2-proxy method").

Response: Thank you for pointing out this ambiguity. We agree that "the proxy-based method" lacks specificity, especially given the preceding mention of "proxy variables". We have revised the text to clarify that the method refers specifically to the estimation of anthropogenic CO_2 emissions using NO_2 as the proxy.

We have corrected the description in the revised manuscript. See Lines 472-474, Page 16.

"This study also estimates anthropogenic CO_2 emissions using a NO_2-proxy method, with monthly CO_2-to-NO_X emission ratios from MEICv2 for December 2022–February 2023 (Fig. 2)."

6. Line 447: "Fig. 4h-i" is referenced, but the Fig. 4 caption only describes panels (a)-(g). Please check and correct the panel labels.

Response: Thank you for pointing out this inconsistency. "Fig. 4h-i" in the main text is a citation error and should be corrected to "Fig. 4d-f", which corresponds to the panels actually discussed at that point in the text. Specifically, Fig. 4d-e show the comparison

of simulated and observed XCO_2 at the XH and HF sites, and Fig. 4f shows the MAE of prior and posterior simulations at the two sites.

We have corrected the citation ("Fig. 4h-i" → "Fig. 4d-f") in the revised manuscript. See Line 573, Page 22.

"The evaluation results at the TCCON sites show that the posterior simulations were consistently improved compared to the prior simulations (Fig. 4d-f)."

7. Line 812: "GenevaWMO-No. 1368". Change to "Geneva, WMO-No. 1368".

Response: We have changed "GenevaWMO-No. 1368" to "Geneva, WMO-No. 1368". See Line 1060, Page 40.

References

Agustí-Panareda, A., Massart, S., Chevallier, F., Boussetta, S., Balsamo, G., Beljaars, A., Ciais, P., Deutscher, N. M., Engelen, R., Jones, L., Kivi, R., Paris, J.-D., Peuch, V.-H., Sherlock, V., Vermeulen, A. T., Wennberg, P. O., and Wunch, D.: Forecasting global atmospheric CO2, Atmos. Chem. Phys., 14, 11959–11983, https://doi.org/10.5194/acp-14-11959-2014, 2014.

Baker, D. F., Bösch, H., Doney, S. C., O'Brien, D., and Schimel, D. S.: Carbon source/sink information provided by column CO2 measurements from the Orbiting Carbon Observatory, Atmos. Chem. Phys., 10, 4145–4165, https://doi.org/10.5194/acp-10-4145-2010, 2010.

Baker, D. F., Bell, E., Davis, K. J., Campbell, J. F., Lin, B., and Dobler, J.: A new exponentially decaying error correlation model for assimilating OCO-2 column-average CO2 data using a length scale computed from airborne lidar measurements, Geosci. Model Dev., 15, 649 – 668, https://doi.org/10.5194/gmd-15-649-2022, 2022.

Basu, S., Baker, D. F., Chevallier, F., Patra, P. K., Liu, J., and Miller, J. B.: The impact of transport model differences on CO2 surface flux estimates from OCO-2 retrievals of column average CO2, Atmos. Chem. Phys., 18, 7189–7215, https://doi.org/10.5194/acp-18-7189-2018, 2018.

Byrne, B., Liu, J., Bowman, K. W., Yin, Y., Yun, J., Ferreira, G. D., Ogle, S. M., Baskaran, L., He, L., Li, X., Xiao, J., and Davis, K. J.: Regional inversion shows promise in capturing extreme-event-driven CO2 flux anomalies but is limited by atmospheric CO2 observational coverage, J. Geophys. Res. Atmos., 129, e2023JD040006, https://doi.org/10.1029/2023JD040006, 2024.

Chen, Z., Jacob, D. J., Nesser, H., Sulprizio, M. P., Lorente, A., Varon, D. J., Lu, X., Shen, L., Qu, Z., Penn, E., and Yu, X.: Methane emissions from China: a high-resolution inversion of TROPOMI satellite observations, Atmos. Chem. Phys., 22, 10809 – 10826, https://doi.org/10.5194/acp-22-10809-2022, 2022.

Chen, Z., Lin, H., Balasus, N., Hardy, A., East, J. D., Zhang, Y., Runkle, B. R. K., Hancock, S. E., Taylor, C. A., Du, X., Sander, B. O., and Jacob, D. J.: Global Rice Paddy Inventory (GRPI): A high-resolution inventory of methane emissions from rice agriculture based on Landsat satellite inundation data, Earth's Future, 13, e2024EF005479, https://doi.org/10.1029/2024EF005479, 2025.

Feng, S., Jiang, F., Zhang, Y., Chen, H., Zhuang, H., Wang, S., Bai, S., Wang, H., and Ju, W.: High-resolution regional inversion reveals overestimation of anthropogenic methane emissions in China, Atmos. Chem. Phys., 25, 15121–15143, https://doi.org/10.5194/acp-25-15121-2025, 2025.

Friedlingstein, P., O'Sullivan, M., Jones, M. W., Andrew, R. M., Bakker, D. C. E., Hauck, J., Landsch ützer, P., Le Quéré, C., Li, H., Luijkx, I. T., Peters, G. P., Peters, W., Pongratz, J., Schwingshackl, C., Sitch, S., Canadell, J. G., Ciais, P., Aas, K., Alin, S. R., Anthoni, P., Barbero, L., Bates, N. R., Bellouin, N., Benoit-Cattin, A., Berghoff, C. F., Bernardello, R., Bopp, L., Brasika, I. B. M., Chamberlain, M. A., Chandra, N., Chevallier, F., Chini, L. P., Collier, N. O., Colligan, T. H., Cronin, M., Djeutchouang, L. M., Dou, X., Enright, M. P., Enyo, K., Erb, M., Evans, W., Feely, R. A., Feng, L., Ford, D. J., Foster, A., Fransner, F., Gasser, T., Gehlen, M., Gkritzalis, T., Goncalves De Souza, J., Grassi, G., Gregor, L., Gruber, N., Guenet, B., Gürses, Ö., Harrington, K., Harris, I., Heinke, J., Hurtt, G. C., Iida, Y., Ilyina, T., Ito, A., Jacobson, A. R., Jain, A. K., Jarníková, T., Jersild, A., Jiang, F., Jones, S. D., Kato, E., Keeling, R. F., Klein Goldewijk, K., Knauer, J., Kong, Y., Korsbakken, J. I., Koven, C., Kunimitsu, T., Lan, X., Liu, J., Liu, Z., Liu, Z., Lo Monaco, C., Ma, L., Marland, G., McGuire, P. C., McKinley, G. A., Melton, J. R., Monacci, N., Monier, E., Morgan, E. J., Munro, D. R., Müller, J. D., Nakaoka, S.-I., Nayagam, L. R., Niwa, Y., Nutzel, T., Olsen, A., Omar, A. M., Pan,

N., Pandey, S., Pierrot, D., Qin, Z., Regnier, P., Rehder, G., Resplandy, L., Roobaert, A., Rosan, T. M., Rödenbeck, C., Schwinger, J., Skjelvan, I., Smallman, T. L., Spada, V., Sreeush, M. G., Sun, Q., Sutton, A. J., Sweeney, C., Swingedouw, D., Séférian, R., Takao, S., Tatebe, H., Tian, H., Tian, X., Tilbrook, B., Tsujino, H., Tubiello, F., van Ooijen, E., van der Werf, G. R., van de Velde, S. J., Walker, A. P., Wanninkhof, R., Yang, X., Yuan, W., Yue, X., and Zeng, J.: Global Carbon Budget 2025, Earth Syst. Sci. Data, 18, 3211–3288, https://doi.org/10.5194/essd-18-3211-2026, 2026.

He, W., Jiang, F., Ju, W., Chevallier, F., Baker, D. F., Wang, J., Wu, M., Johnson, M. S., Philip, S., Wang, H., Bertolacci, M., Liu, Z., Zeng, N., and Chen, J. M.: Improved constraints on the recent terrestrial carbon sink over China by assimilating OCO-2 XCO2 retrievals, J. Geophys. Res. Atmos., 128, e2022JD037773, https://doi.org/10.1029/2022JD037773, 2023.

Jiang, F., Ju, W., He, W., Wu, M., Wang, H., Wang, J., Jia, M., Feng, S., Zhang, L., and Chen, J. M.: A 10-year global monthly averaged terrestrial net ecosystem exchange dataset inferred from the ACOS GOSAT v9 XCO2 retrievals (GCAS2021), Earth Syst. Sci. Data, 14, 3013 – 3037, https://doi.org/10.5194/essd-14-3013-2022, 2022.

Li, H., Zheng, B., Ciais, P., Boersma, K. F., Riess, T. C. V. W., Martin, R. V., Broquet, G., van der A, R., Li, H., Hong, C., Lei, Y., Kong, Y., Zhang, Q., and He, K.: Satellite reveals a steep decline in China's CO2 emissions in early 2022, Sci. Adv., 9, eadg7429, https://doi.org/10.1126/sciadv.Adg 7429, 2023.

Liu, S., Chu, Y., and Hu, J.: Clean air actions and air quality improvements—Beijing-Tianjin-Hebei and surrounding areas, China, 2013 – 2019, China CDC Wkly., 2, 418 – 421, https://doi.org/10.46234/ccdcw2020.107, 2020.

Rodgers, C. D., and Connor, B. J.: Intercomparison of remote sounding instruments, J. Geophys. Res. Atmos., 108, 4116, https://doi.org/10.1029/2002JD002299, 2003.

Zhang, Z., Feng, S., Chen, Y., Liu, Q., Ju, W., Xiao, W., Huang, C., Wang, Y., Wang, H., Jia, M., Wang, X., and Jiang, F.: Development of a regional carbon assimilation system and its application for estimating fossil fuel carbon emissions in the Yangtze River Delta, China, Sci. Total Environ., 957, 177720, https://doi.org/10.1016/j.scitotenv.2024.177720, 2024.

Xu, J., Zhang, Z., Zhao, X., and Cheng, S.: Downward trend of NO2 in the urban areas of Beijing-Tianjin-Hebei region from 2014 to 2020: Comparison of satellite retrievals, ground observations, and emission inventories, Atmos. Environ., 295, 119531, https://doi.org/10.1016/j.atmosenv.2022.119531, 2023.